

Notes on the Weierstrass Elliptic Function

Alain J. Brizard

Department of Physics, Saint Michael's College, Colchester, VT 05439, USA

A consistent notation for the Weierstrass elliptic function $\wp(z; g_2, g_3)$, for $g_2 > 0$ and arbitrary values of g_3 and $\Delta \equiv g_2^3 - 27g_3^2$, is introduced based on the parametric solution for the motion of a particle in a cubic potential. These notes provide a roadmap for the use of **Mathematica** to calculate the half-periods ($\omega_1, \omega_3, \omega_2 \equiv \omega_1 + \omega_3$) of the Weierstrass elliptic function.

I. INTRODUCTION

The present paper introduces a consistent notation for the Weierstrass elliptic function $\wp(z; g_2, g_3)$, the roots ($\mathbf{e}_1, \mathbf{e}_2, \mathbf{e}_3$), and the half-periods ($\omega_1, \omega_3, \omega_2 \equiv \omega_1 + \omega_3$), where each half-period $\omega_k(g_2, g_3)$ and its associated root \mathbf{e}_k satisfy the definition $\wp(\omega_k; g_2, g_3) \equiv \mathbf{e}_k$. The notation for the half-periods ($\omega_1, \omega_2, \omega_3$) depends on the signs of g_3 and the modular discriminant defined as $\Delta \equiv g_2^3 - 27g_3^2$.

The standard notation for the Weierstrass half-periods ($\bar{\omega}_1, \bar{\omega}_2, \bar{\omega}_3$) when $(g_3, \Delta) = (\pm, +)$ follows Refs. [1, 2]. In the case $(g_3, \Delta) = (+, +)$, the half-period $\bar{\omega}_1(g_2, g_3) = \omega$ is real and the half-period $\bar{\omega}_3(g_2, g_3) = \omega' = i|\omega'|$ is imaginary. The half-periods ($\bar{\omega}_1, \bar{\omega}_3, \bar{\omega}_2 \equiv \bar{\omega}_1 + \bar{\omega}_3$), therefore, form a rectangular lattice with the fundamental period parallelogram defined with corners located at $(0, 2\omega, 2\omega', 2\omega + 2\omega')$. When g_3 changes sign, i.e., $(g_3, \Delta) = (-, +)$, the fundamental period parallelogram is rotated clockwise by 90° to a new parallelogram with corners located at $(0, -2i\omega, 2|\omega'|, 2|\omega'| - 2i\omega)$, where we used $-i\omega' = |\omega'|$. The notation for the half-periods ($\omega_1, \omega_3, \omega_2 \equiv \omega_1 + \omega_3$) adopted here will also follow this standard notation when $(g_3, \Delta) = (\pm, +)$.

When Δ changes sign, i.e., $(g_3, \Delta) = (+, -)$, the standard notation [1] states that the half-period $\bar{\omega}_1(g_2, g_3) = \Omega$ is real and the half-period $\bar{\omega}_3(g_2, g_3) = \Omega/2 + \Omega'$ is complex-valued (where Ω' is purely imaginary). The half-periods ($\bar{\omega}_1, \bar{\omega}_3, \bar{\omega}_2 \equiv \bar{\omega}_1 - \bar{\omega}_3$) form a rhombic lattice with the fundamental period parallelogram defined with corners located at $(0, 2\Omega, \Omega + 2\Omega', \Omega - 2\Omega')$. When g_3 changes sign, i.e., $(g_3, \Delta) = (-, -)$, the fundamental period parallelogram is rotated clockwise by 90° to the new fundamental period parallelogram with corners located at $(0, -2i\Omega, 2|\Omega'| - i\Omega, -2|\Omega'| - i\Omega)$, i.e., $\bar{\omega}_2$ is now defined as $\bar{\omega}_2 = \bar{\omega}_3 - \bar{\omega}_1$ when $(g_3, \Delta) = (-, -)$. The new notation for the half-periods ($\omega_1, \omega_2, \omega_3$) adopted here when $(g_3, \Delta) = (\pm, -)$ will instead assume that $\omega_2 \equiv \omega_1 + \omega_3$, as in the standard case $(g_3, \Delta) = (\pm, +)$.

The purpose of the present notes is to introduce a consistent classification of the roots and half-periods based on the orbit solutions derived for all energy levels associated with unbounded and bounded motion in a cubic potential. Additional notes on the analysis of periodic solutions in classical mechanics involving doubly-periodic elliptic functions are presented in Refs. [3–5].

The remainder of this paper is organized as follows. In Sec. II, we introduce a parameterization of the turning points $x_k(\phi)$ for particle motion in a cubic potential based on the definition $g_3(\phi) = \cos \phi \equiv -2E$, where $g_2 = 3$ and E denotes the particle's total energy. In Sec. III, we introduce a consistent formulation of the Weierstrass elliptic function $\wp(z; g_2, g_3)$ associated with the parameterization introduced in Sec. II. In Sec. IV, the Weierstrass orbit solutions (6) are presented for all energy-level classes for the motion in a cubic potential. Lastly, the Jacobi orbit solutions are presented in Sec. V based on connection relations between the Weierstrass and Jacobi elliptic functions.

II. MOTION IN A CUBIC POTENTIAL

We consider the motion of a (unit-mass) particle in the cubic potential

$$V(x) = \frac{3}{2}x - 2x^3, \quad (1)$$

which has an inflection point at $x = 0$, a minimum at $x = -1/2$, with $V(-1/2) = -1/2$ and $V''(-1/2) = 6$ (i.e., $x = -1/2$ is a stable equilibrium point), and a maximum at $x = 1/2$, with $V(1/2) = 1/2$ and $V''(1/2) = -6$ (i.e., $x = 1/2$ is an unstable equilibrium point). The period of small oscillations near the stable equilibrium point at $x = -1/2$ is $2\pi/\sqrt{6}$.

The equation of motion for a particle of unit mass and total energy E is

$$\dot{x}^2 = 2E - 3x + 4x^3 \equiv 4x^3 - g_2x - g_3, \quad (2)$$

where $\dot{x} = dx/dt$ denotes the particle velocity. The right side of Eq. (2) is expressed in the Weierstrass standard form with the invariants $g_2 = 3$ and $g_3 = -2E$, where bounded and unbounded orbit solutions are classified according to four energy levels summarized in Table I. The total energy $E \equiv -\frac{1}{2} \cos \phi$ is defined in terms of the Weierstrass phase ϕ , which is defined along a continuous path in the complex- ϕ plane:

$$\phi = \begin{cases} -i\psi & (\psi \geq 0) \\ \varphi & (0 \leq \varphi \leq \pi/2) \\ \pi - \varphi & (0 \leq \varphi \leq \pi/2) \\ \pi + i\psi & (\psi \geq 0) \end{cases} \quad (3)$$

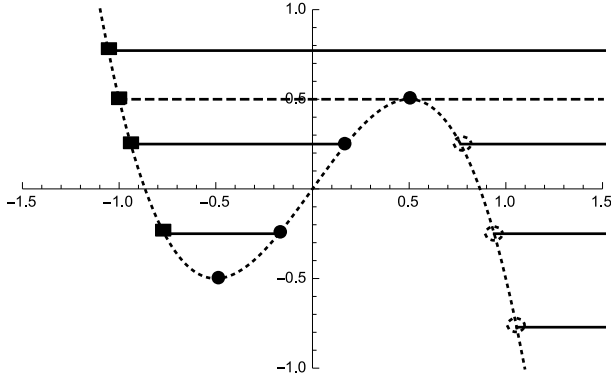


FIG. 1: Energy levels for the particle orbits in the cubic potential (1), shown here as a dotted curve. Solid squares represent the locations of the root $x_3(\phi)$, solid circles represent the locations of the root $x_2(\phi)$, and open circles represent the locations of the root $x_1(\phi)$. The energy level ($E = 1/2$) labeled by a dashed line denotes the bounded and unbounded separatrix orbits.

TABLE I: Energy levels $E = -\frac{1}{2} \cos \phi$ defined in terms of the Weierstrass phase (3).

Energy Levels	ϕ	$E = -\frac{1}{2} \cos \phi$
(I)	$-i\psi$	$E = -\frac{1}{2} \cosh \psi \leq -\frac{1}{2}$
(II)	φ	$-\frac{1}{2} \leq E = -\frac{1}{2} \cos \varphi \leq 0$
(III)	$\pi - \varphi$	$0 \leq E = \frac{1}{2} \cos \varphi \leq \frac{1}{2}$
(IV)	$\pi + i\psi$	$E = \frac{1}{2} \cosh \psi \geq \frac{1}{2}$

which allows us to go continuously from $E < -1/2$ (lowest energy level in Fig. 1) to $E > 1/2$ (highest energy level in Fig. 1).

The turning points (x_1, x_2, x_3) , where the velocity \dot{x} vanishes in Eq. (2), are defined as the roots of the energy equation $E = -\frac{1}{2} \cos \phi = V(x)$:

$$\left. \begin{aligned} x_1(\phi) &= \cos(\phi/3) \\ x_2(\phi) &= -\cos[(\pi + \phi)/3] \\ x_3(\phi) &= -\cos[(\pi - \phi)/3] \end{aligned} \right\}, \quad (4)$$

which satisfy the condition $x_1 + x_2 + x_3 = 0$. The turning points (4) are shown in Table II (as well as Figs. 1 and 2) for each energy region defined in Table I. The equation of motion (2) can, therefore, also be expressed as

$$\dot{x}^2 \equiv 4(x - x_1)(x - x_2)(x - x_3), \quad (5)$$

with the roots defined in Eq. (4).

The orbit solutions for Eq. (2) are expressed in terms of the Weierstrass elliptic function

$$x(t; x_0) = \wp(t + \gamma; 3, \cos \phi), \quad (6)$$

where the constant $\gamma(g_2, g_3; \Delta)$ is determined from the initial condition

$$x_0(\phi) = \wp(\gamma; 3, \cos \phi). \quad (7)$$

TABLE II: Turning points $x_k(\phi)$ defined in Eq. (4).

Energy	$x_1(\phi)$	$x_2(\phi)$	$x_3(\phi)$
(I)	$\cosh(\psi/3)$	$-\cos[(\pi - i\psi)/3]$	$-\cos[(\pi + i\psi)/3]$
(II)	$\cos(\varphi/3)$	$-\cos[(\pi + \varphi)/3]$	$-\cos[(\pi - \varphi)/3]$
(III)	$\cos[(\pi - \varphi)/3]$	$\cos[(\pi + \varphi)/3]$	$-\cos(\varphi/3)$
(IV)	$\cos[(\pi + i\psi)/3]$	$\cos[(\pi - i\psi)/3]$	$-\cosh(\psi/3)$

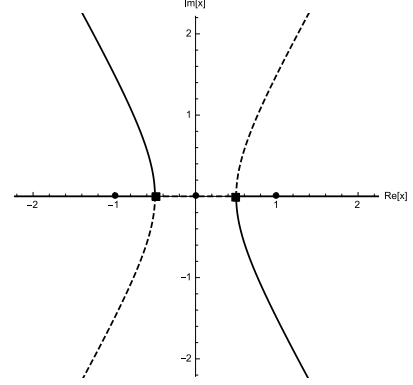


FIG. 2: Graphs of the roots (x_1, x_2, x_3) defined in Eq. (4) and shown in Table II. The real and imaginary parts of $x_1(\phi)$ and $x_3(\phi)$ are shown as solid curves while the real and imaginary parts of $x_2(\phi)$ are shown as dashed curves. In region (I), $x_1 > 1$ is real and $x_2 = x_3^* = a - ib$, with $a < -1/2$. In regions (II)-(III), all roots are real, with $-1 < x_3 < x_2 < x_1 < 1$, and x_2 and x_3 have opposite signs. In region (IV), $x_3 < -1$ is real and $x_1 = x_2^* = a - ib$, with $a > 1/2$. The symmetry properties (9) are clearly apparent with $x_2(\phi)$ and $\text{Im}(x_1) = -\text{Im}(x_3) \leq 0$.

When the motion is periodic, the period $2\omega_k(g_2, g_3)$ depends on $g_2 = 3$, $g_3 = \cos \phi$, and the sign of the modular discriminant $\Delta \equiv g_2^3 - 27g_3^2$:

$$\Delta = 27 \sin^2 \phi = \begin{cases} -27 \sinh^2 \psi \leq 0 & (|E| \geq 1/2) \\ 27 \sin^2 \varphi \geq 0 & (|E| \leq 1/2) \end{cases}$$

Here, the half-periods $\omega_k = (\omega_1, \omega_2 \equiv \omega_1 + \omega_3, \omega_3)$ satisfy the definition

$$\wp(\omega_k; 3, \cos \phi) \equiv x_k(\phi). \quad (8)$$

Figure 2 shows the roots (4), which are also shown in Table II. In region (I), where $E < -1/2$, we note that $x_1^I > 1$ and $x_2^I = x_3^{I*}$. In regions (II)-(III), where $-1/2 < E < 1/2$, the three turning points are real, with $x_3 < x_2 < x_1$. In region (IV), where $E > 1/2$, we note that $x_3^{IV} < -1$ and $x_1^{IV} = x_2^{IV*}$. Moreover, in Table II, we observe the following symmetry properties (see Fig. 2)

$$\left. \begin{aligned} x_2^I &= -x_2^{IV} & \text{and} & & x_2^{II} &= -x_2^{III} \\ x_1^I &= -x_3^{IV} & \text{and} & & x_1^{II} &= -x_3^{III} \end{aligned} \right\}. \quad (9)$$

Lastly, we note that bounded periodic motion exists between the turning points $x_3 < x_2$ only for the energy levels $|E| < 1/2$.

III. WEIERSTRASS ELLIPTIC FUNCTION

Before finding explicit expressions for the solutions (6), we need to explore the properties of the Weierstrass elliptic function $\wp(z; g_2, g_3)$, with the invariants $(g_2, g_3; \Delta)$ defined as

$$\left. \begin{aligned} g_2 &= 3\beta^2 \\ g_3 &= \beta^3 \cos\phi \\ \Delta &= g_2^3 - 27g_3^2 = 27\beta^6 \sin^2\phi \end{aligned} \right\}, \quad (10)$$

where β is an arbitrary (real or complex) parameter and the phase ϕ may be real or complex. The differential equation for the Weierstrass elliptic function $w \equiv \wp(z; g_2, g_3)$ is

$$\left(\frac{dw}{dz}\right)^2 = 4w^3 - g_2w - g_3 \equiv P(w), \quad (11)$$

where the cubic polynomial $P(w)$ has three roots (e_1, e_2, e_3) defined as

$$\left. \begin{aligned} e_1(\phi) &= \beta \cos(\phi/3) \\ e_2(\phi) &= -\beta \cos[(\pi + \phi)/3] \\ e_3(\phi) &= -\beta \cos[(\pi - \phi)/3] \end{aligned} \right\}, \quad (12)$$

where we used the definitions (10). The roots (4) are, of course, obtained from Eq. (12) through the identity $x_k(\phi) \equiv e_k(\phi)/\beta$.

The polynomial $P(w) = 4w^3 - g_2w - g_3$ has a minimum at $w = \sqrt{g_2/12} \equiv w_0$ and a maximum at $w = -\sqrt{g_2/12} = -w_0$, where $P(\pm w_0) = \mp\sqrt{g_2^3/27} - g_3$. We note that the extrema $\pm w_0$ are real only if $g_2 > 0$ and g_3 is real. Hence, using the discriminant $\Delta \equiv g_2^3 - 27g_3^2$, the maximum $P(-w_0) = \sqrt{g_2^3 + \Delta/27} - g_3 > 0$ if $\Delta > 0$, and the three roots (12) are real when $g_3 > 0$. When $g_3 < 0$, on the other hand, the minimum $P(w_0) = -\sqrt{g_2^3 + \Delta/27} + |g_3| < 0$ if $\Delta > 0$ and the three roots (12) are once again real. Lastly, only one root is real when $\Delta < 0$: e_1 is real when $g_3 > 0$ (with $e_2 = e_3^*$) or e_3 is real when $g_3 < 0$ (with $e_1 = e_2^*$).

A. Inversion formulas

Equation (11) can be transformed as

$$\begin{aligned} \lambda^6 \left(\frac{dw}{dz}\right)^2 &= \left[\frac{d(\lambda^2 w)}{d(z/\lambda)}\right]^2 \\ &= 4(\lambda^2 w)^3 - (\lambda^4 g_2)(\lambda^2 w) - (\lambda^6 g_3) \\ &\equiv \left(\frac{d\bar{w}}{d\tau}\right)^2 = 4\bar{w}^3 - \bar{g}_2 \bar{w} - \bar{g}_3, \end{aligned}$$

where $\bar{w} \equiv \lambda^2 w$ and $\tau \equiv z/\lambda$. Since \bar{w} has the Weierstrass solution

$$\begin{aligned} \bar{w}(\tau) &= \wp(\tau; \bar{g}_2, \bar{g}_3) = \wp\left(\lambda^{-1}z; \lambda^4 g_2, \lambda^6 g_3\right) \\ &\equiv \lambda^2 \wp(z; g_2, g_3), \end{aligned}$$

we obtain the identity

$$\wp(z; g_2, g_3) \equiv \lambda^{-2} \wp\left(\lambda^{-1}z; \lambda^4 g_2, \lambda^6 g_3\right). \quad (13)$$

Hence, if $\lambda = -1$, the Weierstrass elliptic function is shown to have even parity:

$$\wp(-z; g_2, g_3) = \wp(z; g_2, g_3). \quad (14)$$

Next, if $\lambda = -i$, we find the g_3 -inversion formula

$$\wp\left(z; g_2, g_3\right) \equiv -\wp(iz; g_2, |g_3|). \quad (15)$$

The g_2 -inversion formula, on the other hand, is obtained with $\lambda = \exp(-i\pi/4)$ so that

$$\wp(z; g_2, g_3) \equiv i\wp\left(e^{i\pi/4}z; |g_2|, i|g_3|\right). \quad (16)$$

Lastly, by substituting $\lambda \equiv \beta^{1/2}$ into Eq. (13), we find

$$\wp(t + \gamma; 3, \cos\phi) \equiv \beta^{-1} \wp\left(\beta^{-1/2}(t + \gamma); g_2, g_3\right), \quad (17)$$

where (g_2, g_3) are given by Eq. (10). Hence, the general orbit solution (6) can be mapped into the general solution $\wp(z; g_2, g_3)$ for the Weierstrass differential equation (11), with $z \equiv \beta^{-1/2}(t + \gamma)$.

B. Weierstrass Half-periods

We now explore the half-periods $\omega_1(g_2, g_3)$ and $\omega_3(g_2, g_3)$ for $g_2 > 0$ and the four sign-pairings for (g_3, Δ) shown in Table III. Here, the half-periods ω and Ω are real, and the half-periods $\omega' = i|\omega'|$ and $\Omega' = i|\Omega'|$ are imaginary. When $g_2 = 3\beta^2$ and $g_3 = \beta^3 > 0$, so that $\Delta = 0$, we find

$$\omega(3\beta^2, \beta^3) = \Omega(3\beta^2, \beta^3) = \frac{\pi}{\sqrt{6}\beta} \equiv \Omega_0 \quad (18)$$

and $\omega' = \Omega' = i\infty$. When $g_2 = 3\beta^2$ and $g_3 = 0$, we find

$$\omega(3\beta^2, 0) = \frac{K(1/2)}{(3\beta^2)^{1/4}} \equiv \omega_0, \quad (19)$$

where $K(m)$ denotes the complete elliptic integral of the first kind.

Figure 3 compares the new fundamental period parallelogram (shown as a solid rhombus) for the case $(g_3, \Delta) = (+, -)$ with the standard fundamental period

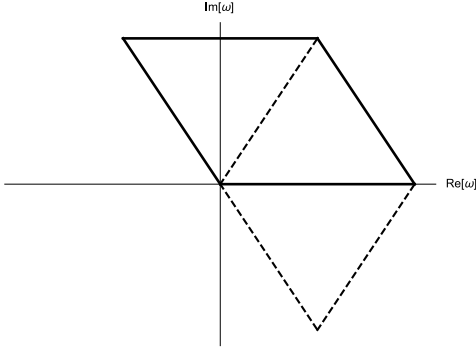


FIG. 3: New fundamental period parallelogram (20), shown as a solid rhombus with corners located at $(0, 2\Omega, -\Omega + 2\Omega', \Omega + 2\Omega')$, and standard fundamental period parallelogram (21), shown as a dashed rhombus with corners located at $(0, 2\Omega, \Omega + 2\Omega', \Omega - 2\Omega')$, for the case $(g_3, \Delta) = (+, -)$. Here, Ω is purely real and Ω' is purely imaginary.

TABLE III: Half-periods $\omega_1(g_2, g_3)$ and $\omega_3(g_2, g_3)$ for $g_2 = 3\beta^2$, $g_3 = \beta^3 \cos \phi$, and $\Delta = 27\beta^6 \sin^2 \phi$, with $\omega_2 \equiv \omega_1 + \omega_3$.

	(g_3, Δ)	ω_1	ω_3	ω_2
(I)	$(+, -)$	Ω	$-\Omega/2 + \Omega'$	$\Omega/2 + \Omega'$
	$(+, 0)$	Ω_0	$i\infty$	$i\infty$
(II)	$(+, +)$	ω	ω'	$\omega + \omega'$
	$(0, +)$	ω_0	$i\omega_0$	$(1 + i)\omega_0$
(III)	$(-, +)$	$-i\omega' = \omega' $	$-i\omega$	$ \omega' - i\omega$
	$(-, 0)$	∞	$-i\Omega_0$	∞
(IV)	$(-, -)$	$ \Omega' + i\Omega/2$	$-i\Omega$	$ \Omega' - i\Omega/2$

parallelogram (shown as a dashed rhombus) as defined in Ref. [1]. The corners of the new rhombus are located at

$$(0, 2\omega_1, 2\omega_3, 2\omega_2) = (0, 2\Omega, -\Omega + 2\Omega', \Omega + 2\Omega'), \quad (20)$$

where $\omega_2 \equiv \omega_1 + \omega_3$, while the corners of the standard rhombus are located at

$$(0, 2\bar{\omega}_1, 2\bar{\omega}_3, 2\bar{\omega}_2) = (0, 2\Omega, \Omega + 2\Omega', \Omega - 2\Omega'), \quad (21)$$

where $\bar{\omega}_2 \equiv \bar{\omega}_1 - \bar{\omega}_3$. Hence, we immediately see that both fundamental period parallelograms identify $\omega_1 = \Omega = \bar{\omega}_1$ as real, while the new fundamental period parallelogram identifies the new half-period ω_2 as the standard half-period $\bar{\omega}_3$ in the standard fundamental period parallelogram. We note that the standard half-periods $(\bar{\omega}_2, \bar{\omega}_3)$ satisfy $\bar{\omega}_2 \equiv \bar{\omega}_1 - \bar{\omega}_3 = \bar{\omega}_3^*$, while the new half-periods (ω_2, ω_3) satisfy $\omega_2 \equiv \omega_1 + \omega_3 = -\omega_3^*$. Both definitions satisfy the relations $\mathbf{e}_2 = \wp(\bar{\omega}_2; g_2, g_3) = [\wp(\bar{\omega}_3; g_2, g_3)]^* = \mathbf{e}_3^*$ and $\mathbf{e}_2 = \wp(\omega_2; g_2, g_3) = [\wp(-\omega_3; g_2, g_3)]^* = \mathbf{e}_3^*$, which follows from the fact that the Weierstrass elliptic function has even parity, i.e., $\wp(-\omega_3) = \wp(\omega_3)$. The advantage of the new definition of ω_2 is that it is consistently defined as $\omega_2 \equiv \omega_1 + \omega_3$ for all values of (g_3, Δ) .

The definitions in Table III for the half-periods satisfy Eq. (8), while the symmetry properties associated with

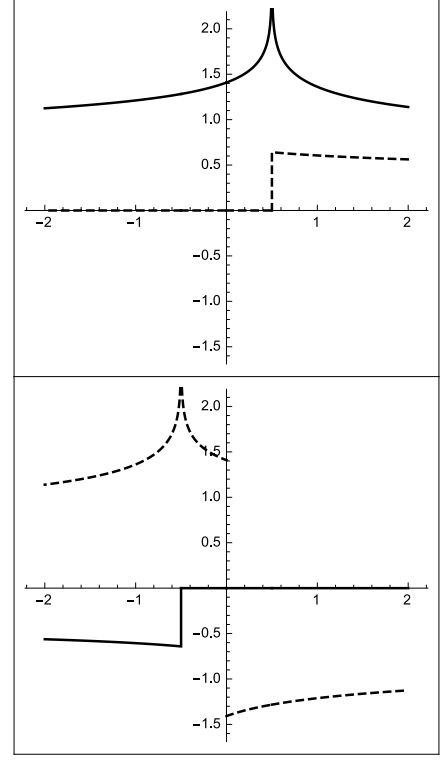


FIG. 4: Plots of ω_1 (top; real part = solid and imaginary part = dashed), Eq. (28), and ω_3 (bottom; real part = solid and imaginary part = dashed), Eq. (29), as functions of energy $-2 \leq E = -g_3/2 \leq 2$, with $\beta = 1$ in Eqs. (10) and (12). When g_3 changes sign, $\omega_1^+ = \Omega$ ($E \leq -1/2$) or $\omega_1^- = \omega$ ($-1/2 \leq E \leq 0$) transforms into $\omega_3^- = -i\omega_1^+ = -i\omega$ ($0 \leq E \leq 1/2$) or $\omega_3^+ = -i\Omega$ ($E \geq 1/2$), while $\omega_3^+ = -\Omega/2 + \Omega'$ ($E \leq -1/2$) or $\omega_3^- = \omega'$ ($-1/2 \leq E \leq 0$) transforms into $\omega_1^- = -i\omega_3^+ = |\omega'|$ ($0 \leq E \leq 1/2$) or $\omega_1^+ = i\Omega/2 + |\Omega'|$ ($E \geq 1/2$).

the sign inversion for g_3 (for $g_2 > 0$) are satisfied by Eq. (15) between $(g_3, \Delta) = (\pm, -)$ in regions (I) and (IV):

$$\begin{aligned} \mathbf{e}_1^- &= \wp(|\Omega'| + i\Omega/2; g_2, g_3 < 0) \\ &= -\wp(\Omega' - \Omega/2; g_2, |g_3|) = -\mathbf{e}_3^+, \end{aligned} \quad (22)$$

$$\begin{aligned} \mathbf{e}_2^- &= \wp(|\Omega'| - i\Omega/2; g_2, g_3 < 0) \\ &= -\wp(\Omega' + \Omega/2; g_2, |g_3|) = -\mathbf{e}_2^+, \end{aligned} \quad (23)$$

$$\begin{aligned} \mathbf{e}_3^- &= \wp(-i\Omega; g_2, g_3 < 0) \\ &= -\wp(\Omega; g_2, |g_3|) = -\mathbf{e}_1^+, \end{aligned} \quad (24)$$

and $(g_3, \Delta) = (\pm, +)$ in regions (II) and (III):

$$\begin{aligned} \mathbf{e}_1^- &= \wp(|\omega'|; g_2, g_3 < 0) \\ &= -\wp(\omega'; g_2, |g_3|) = -\mathbf{e}_3^+, \end{aligned} \quad (25)$$

$$\begin{aligned} \mathbf{e}_2^- &= \wp(|\omega'| - i\omega; g_2, g_3 < 0) \\ &= -\wp(\omega' + \omega; g_2, |g_3|) = -\mathbf{e}_2^+, \end{aligned} \quad (26)$$

$$\begin{aligned} \mathbf{e}_3^- &= \wp(-i\omega; g_2, g_3 < 0) \\ &= -\wp(\omega; g_2, |g_3|) = -\mathbf{e}_1^+. \end{aligned} \quad (27)$$

From Eqs. (22)-(24), we immediately observe that

$(e_1^-)^* = e_2^-$ and $(e_3^+)^* = e_2^+$, while $e_3^- = -e_1^+$ are purely real.

Lastly, the direct calculations of the half-periods $\omega_1(g_2, g_3)$ and $\omega_3(g_2, g_3)$ are given in terms of the integrals [1]

$$\omega_1^\pm(g_2, g_3) = \int_{e_1^\pm}^{\infty} \frac{dw}{\sqrt{P_\pm(w)}}, \quad (28)$$

$$\omega_3^\pm(g_2, g_3) = \pm i \int_{-\infty}^{e_3^\pm} \frac{dw}{\sqrt{|P_\pm(w)|}}, \quad (29)$$

where the sign \pm in Eqs. (28)-(29) is determined by the sign of g_3 , $P_\pm(w) \equiv 4(w - e_1^\pm)(w - e_2^\pm)(w - e_3^\pm)$, and the roots $(e_1^\pm, e_2^\pm, e_3^\pm)$ are defined in Eq. (12) in terms of the phase ϕ . The half-periods (28)-(29), which are shown in Fig. 4, satisfy the g_3 -inversion relations

$$\begin{aligned} \omega_3^- &= -i \int_{-\infty}^{e_3^-} \frac{dw}{\sqrt{|P_-(w)|}} = -i \int_{-\infty}^{-e_1^+} \frac{dw}{\sqrt{|P_-(w)|}} \\ &= -i \int_{e_1^+}^{\infty} \frac{dw}{\sqrt{P_+(w)}} = -i\omega_1^+, \end{aligned} \quad (30)$$

$$\begin{aligned} \omega_1^- &= \int_{e_1^-}^{\infty} \frac{dw}{\sqrt{P_-(w)}} = \int_{-e_3^+}^{\infty} \frac{dw}{\sqrt{P_-(w)}} \\ &= \int_{-\infty}^{e_3^+} \frac{dw}{\sqrt{|P_+(w)|}} = -i\omega_3^+, \end{aligned} \quad (31)$$

where we used the relations (22)-(27), with the identity $P_-(-w) \equiv -P_+(w)$. We note that $P_+(w) > 0$ in Eq. (30) for $w > e_1^+$, while $P_+(w) < 0$ in Eq. (31) for $w < e_3^+$, so that $P_-(-w) \equiv -P_+(w) = |P_+(w)|$. The half-periods $\omega_2^\pm \equiv \omega_1^\pm + \omega_3^\pm$ are consistently defined in terms of Eqs. (28)-(29), with $\omega_2^- = -i\omega_2^+$.

C. Mathematica outputs

Table IV and Fig. 5 show the outputs of the function $\text{WeierstrassHalfPeriods}(g_2, g_3) = \{\omega_a, \omega_b\}$ from Mathematica. Here, the first output ω_a is either ω_1^+ if $E \leq 0$ or $\omega_3^- = -i\omega_1^+$ if $E > 0$. The second output ω_b , on the other hand, is either ω_2^\pm if $|E| > 1/2$ or ω_3^\pm and $\omega_1^- = -i\omega_3^\pm$ if $|E| < 1/2$. The definitions of $(\omega_1^\pm, \omega_3^\pm, \omega_2^\pm \equiv \omega_1^\pm + \omega_3^\pm)$ follow the notation presented in Table III.

We note that, while Mathematica's output ω_a is well behaved for all values of E , the output ω_b is stable only when $|E| \leq 1/2$. When $|E| > 1/2$, however, the output ω_b appears unstable and oscillates between $\omega_2^I = \Omega/2 + \Omega'$ and $\omega_3^I = -\Omega/2 + \Omega'$ when $E < -1/2$, where the imaginary part Ω' is stable but the real part oscillates between $\pm\Omega/2$, and $\omega_2^{IV} = -i\Omega/2 + |\Omega'|$ and $\omega_1^{IV} = i\Omega/2 + |\Omega'|$ when $E > 1/2$, where the real part $|\Omega'|$ is stable but the imaginary part oscillates between $\pm i\Omega/2$.

The source of this unstable behavior for ω_b in regions (I) and (IV), where $|E| > 1/2$, is unclear so Table IV can be used for a consistent calculation of the half-periods in

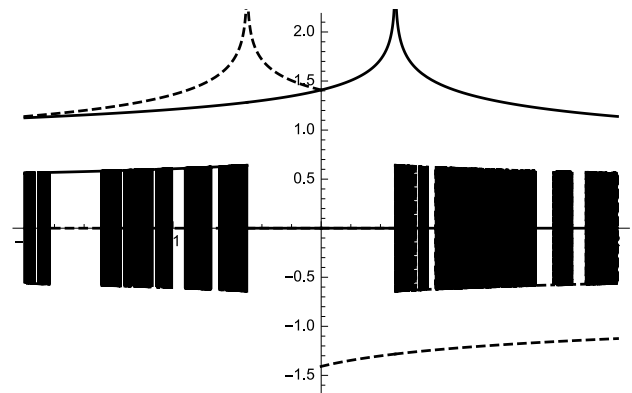


FIG. 5: Plots of Mathematica real (solid) and imaginary (dashed) outputs $\{\omega_a, \omega_b\} = \text{WeierstrassHalfPeriods}(g_2, g_3)$.

TABLE IV: $\text{WeierstrassHalfPeriods}(g_2, g_3) = \{\omega_a, \omega_b\}$ as calculated by Mathematica.

	(g_3, Δ)	ω_a	ω_b
(I)	$(+, -)$	$\omega_1 = \Omega$	$\omega_2 = \Omega/2 + \Omega'$
	$(+, 0)$	Ω_0	$i\infty$
(II)	$(+, +)$	$\omega_1 = \omega$	$\omega_3 = \omega'$
	$(0, +)$	ω_0	$i\omega_0$
(III)	$(-, +)$	$\omega_3 = -i\omega$	$\omega_1 = -i\omega' = \omega' $
	$(-, 0)$	$-i\Omega_0$	∞
(IV)	$(-, -)$	$\omega_3 = -i\Omega$	$\omega_2 = \Omega' - i\Omega/2$

regions (I) and (IV). We note, however, that this instability does not affect the identity $x_2^I = x_3^{I*}$ in region (I) and the identity $x_2^{IV} = x_1^{IV*}$ in region (IV).

IV. WEIERSTRASS ORBIT SOLUTIONS

We now express the orbit solutions (6) for each of the four energy-level regions shown in Table I. These orbit solutions are shown in Fig. 6.

A. Orbits in Region (I)

For region (I), with energy levels $E < -1/2$ and $(g_3, \Delta) = (+, -)$, only unbounded (u) motion is possible since $x_1^I > 1$ is real and $x_2^I = x_3^{I*}$ are complex-conjugate. Using the initial condition $x_I^u(0) = x_1^I$ and $\omega_1^I = \Omega$ from Table III, we find

$$x_I^u(t) = \wp(t + \omega_1^I; g_2, g_3) = \wp(t + \Omega; g_2, g_3). \quad (32)$$

Since Ω is real and $\wp(2\Omega; g_2, g_3) = \wp(0; g_2, g_3) = \infty$, then the complete unbounded orbit $x_I^u(t)$ can be mapped out for $-\Omega < t < \Omega$.

B. Orbits in Region (II)

For region (II), with energy levels $-1/2 < E < 0$ and $(g_3, \Delta) = (+, +)$, unbounded (u) and bounded (b) motions are possible for $x_{II}^u > x_1^{II}$ and between $x_3^{II} < x_{II}^b < x_2^{II} < 0$.

For the bounded-motion solution, using the initial condition $x_{II}^b(0) = x_3^{II}$ and $\omega_3^{II} = \omega'$ from Table III, we find the periodic solution

$$\begin{aligned} x_{II}^b(t) &= \wp\left(t + \omega_3^{II}; g_2, g_3\right) \\ &= \wp\left(t + \omega'; g_2, g_3\right), \end{aligned} \quad (33)$$

with a period $2\omega_1^{II} = 2\omega$, so the bounded orbit $x_{II}^b(t)$ can be mapped out for $0 \leq t \leq 2\omega$. At the half-period $t = \omega_1^{II} = \omega$, we find

$$\begin{aligned} x_{II}^b(\omega_1^{II}) &= \wp\left(\omega_1^{II} + \omega_3^{II}; g_2, g_3\right) \\ &= \wp\left(\omega_2^{II}; g_2, g_3\right) = x_2^{II}. \end{aligned} \quad (34)$$

We note that as the energy level approaches $E = -1/2$ (from above), the period approaches $2\Omega_0 = 2\pi/\sqrt{6}$, which is the expected period of small oscillations in the vicinity of the stable equilibrium point at $x = -1/2$, where $V''(-1/2) = 6$. The bounded-motion solution (33) approaches $x_{II}^b(t) \rightarrow -1/2$ as $\omega' \rightarrow i\infty$.

For the unbounded-motion solution, using the initial condition $x_{II}^u(0) = x_1^{II}$ and $\omega_1^{II} = \omega$ from Table III, we find

$$x_{II}^u(t) = \wp\left(t + \omega_1^{II}; g_2, g_3\right) = \wp\left(t + \omega; g_2, g_3\right). \quad (35)$$

Once again, since ω is real and $\wp(2\omega; g_2, g_3) = \wp(0; g_2, g_3) = \infty$, then the complete unbounded orbit $x_{II}^u(t)$ can be mapped out for $-\omega < t < \omega$.

C. Orbits in Region (III)

For region (III), with energy levels $0 < E < 1/2$ and $(g_3, \Delta) = (-, +)$, unbounded (u) and bounded (b) motions are possible for $x_{III}^u > x_1^{III}$ and between $x_3^{III} < x_{III}^b < x_2^{III}$, where $x_3^{III} < 0$ and $x_2^{III} > 0$.

For the bounded-motion solution, using the initial condition $x_{III}^b(0) = x_3^{III}$ and $\omega_3^{III} = -i\omega$ from Table III, we find the periodic solution

$$\begin{aligned} x_{III}^b(t) &= \wp\left(t + \omega_3^{III}; g_2, g_3\right) = \wp\left(t - i\omega; g_2, g_3\right) \\ &= -\wp\left(it + \omega; g_2, |g_3|\right), \end{aligned} \quad (36)$$

where we used the inversion formula (15). This bounded solution has the period $2\omega_1^{III} = 2|\omega'|$, so the bounded orbit $x_{III}^b(t)$ can be mapped out for $0 \leq t \leq 2|\omega'|$. At at

the half-period $t = \omega_1^{III} = |\omega'|$, we find

$$\begin{aligned} x_{III}^b(\omega_1^{III}) &= \wp\left(\omega_1^{III} + \omega_3^{III}; g_2, g_3\right) \\ &= \wp\left(\omega_2^{III}; g_2, g_3\right) = x_2^{III}. \end{aligned} \quad (37)$$

We note that as the energy level approaches $E = 1/2$ (from below), the period approaches $2|\omega'| \rightarrow \infty$ while the bounded-motion solution (36) approaches the separatrix solution (with $g_3 = -1$ and $\Delta = 0$)

$$\begin{aligned} x_{III}^{bs}(t) &= \wp\left(t - i\Omega_0; 3, -1\right) \\ &= -1 + \frac{3}{2} \coth^2\left(\sqrt{\frac{3}{2}}(t - i\Omega_0)\right), \end{aligned} \quad (38)$$

where $\Omega_0 = \pi/\sqrt{6}$. Here, we recover

$$x_{III}^{bs}(0) = -1 + \frac{3}{2} \coth^2\left(-i\frac{\pi}{2}\right) = -1$$

and, as $t \rightarrow \infty$, we find $x_{III}^{bs}(t) \rightarrow -1 + 3/2 = 1/2$.

For the unbounded-motion solution, using the initial condition $x_{III}^u(0) = x_1^{III}$ and $\omega_1^{III} = -i\omega' = |\omega'|$ from Table III, we find

$$\begin{aligned} x_{III}^u(t) &= \wp\left(t + \omega_1^{III}; g_2, g_3\right) = \wp\left(t + |\omega'|; g_2, g_3\right) \\ &= -\wp\left(it + \omega'; g_2, |g_3|\right), \end{aligned} \quad (39)$$

where we used the inversion formula (15). Once again, since $|\omega'|$ is real and $\wp(2\omega'; g_2, |g_3|) = \wp(0; g_2, |g_3|) = \infty$, then the complete unbounded orbit $x_{III}^u(t)$ can be mapped out for $-|\omega'| < t < |\omega'|$.

The unbounded separatrix solution $x_{III}^{bu}(t)$ may be obtained from a slight modification of the unbounded solution (39). First, we define the new unbounded solution in region (III) to be

$$x_{III}^u(t) = \wp\left(t; g_2, g_3\right) = -\wp\left(it; g_2, |g_3|\right), \quad (40)$$

which assumes that $x_{III}^u(0) = \infty$ and

$$x_{III}^u(|\omega'|) = \wp\left(|\omega'|; g_2, g_3\right) = x_1^{III}.$$

The unbounded separatrix solution may be written as

$$x_{III}^{us}(t) = -1 + \frac{3}{2} \coth^2\left(\sqrt{\frac{3}{2}}t\right), \quad (41)$$

where $x_{III}^{us}(0) = \infty$ and $x_{III}^{us}(\infty) = -1 + 3/2 = 1/2$.

D. Orbits in Region (IV)

Lastly, for region (IV), with energy levels $E > 1/2$ and $(g_3, \Delta) = (-, -)$, only unbounded (u) motion is possible

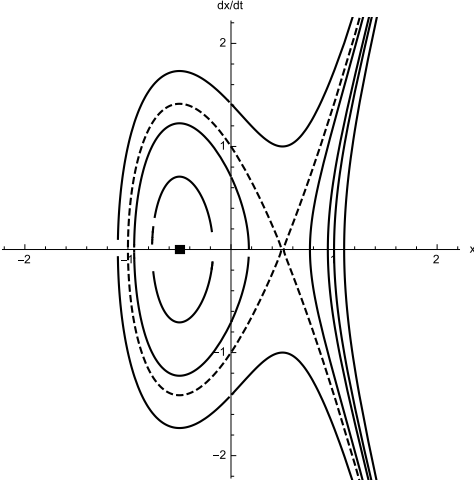


FIG. 6: Phase plot $(x, dx/dt)$ for the Weierstrass unbounded and bounded orbit solutions. The bounded and unbounded separatrix solutions are shown as dashed curves and the square dot denotes the stable equilibrium point at $x = -1/2$.

since $x_3^{IV} < -1$ is real and $x_1^{IV} = x_2^{IV*}$ are complex-conjugate. Using the initial condition $x_{IV}^u(0) = x_3^{IV} = -x_1^I$ and $\omega_3^{IV} = -i\Omega$ from Table III, we find

$$\begin{aligned} x_{IV}^u(t) &= \wp\left(t + \omega_3^{IV}; g_2, g_3\right) = \wp\left(t - i\Omega; g_2, g_3\right) \\ &= -\wp\left(\Omega + it; g_2, |g_3|\right), \end{aligned} \quad (42)$$

where we used the inversion formula (15). We note that at $t = 2|\Omega'| \equiv \omega_1^{IV} + \omega_2^{IV}$, or $it = 2\Omega'$, we find

$$\begin{aligned} x_{IV}^u(2|\Omega'|) &= -\wp\left(\Omega + 2\Omega'; g_2, |g_3|\right) \\ &= -\wp\left(2\omega_2^I; g_2, |g_3|\right) = -(-\infty) = \infty, \end{aligned} \quad (43)$$

so that the complete unbounded orbit $x_{IV}^u(t)$ can be mapped out for $-2|\Omega'| < t < 2|\Omega'|$.

E. Weierstrass orbit solutions

The Weierstrass orbit solutions are shown in Fig. 6, with the bounded and unbounded separatrix solutions (for $g_3 = -1$ and $\Delta = 0$) shown as dashed curves. Solutions found inside the bounded separatrix solution are the bounded solutions (33) and (36), while solutions found outside are the unbounded solutions (32), (35), (39), and (42). The bounded solution (33) in region (II) is periodic between $x_3^{II} < x_2^{II} < 0$, while the bounded solution (36) in region (III) is periodic between $x_3^{III} < 0 < x_2^{III}$. The unbounded solutions [(32), (35), (39)] in regions (I)-(III) have a turning points at $0 < x_1^{III} < x_1^{II} < x_1^I$, while the unbounded solution (42) in region (IV) has a turning point at $x_3^{IV} < 0$. Lastly, the potential (1) has stable equilibrium point at $x = -1/2$ (shown as a square dot in Fig. 6) and an unstable equilibrium point $x = 1/2$, shown

in Fig. 6 as the point where the bounded and unbounded separatrix solutions cross.

Lastly, by using the g_3 -inversion formula (15), we observe the following relations between bounded and unbounded orbit solutions

$$\left. \begin{aligned} x_{II}^b(t) &= -x_{III}^u(it) \\ x_{III}^b(t) &= -x_{II}^u(it) \\ x_{IV}^u(t) &= -x_I^u(it) \end{aligned} \right\}. \quad (44)$$

Hence, bounded motion can be viewed in terms of unbounded motion in imaginary time.

V. JACOBI ORBIT SOLUTIONS

In this last Section, we proceed with the transformation of our Weierstrass orbit solutions into expressions involving the Jacobi elliptic functions [6] $\text{cn}(z|m)$, $\text{sn}(z|m)$, and $\text{dn}(z|m)$, where $z(t; \phi) = \kappa(\phi)t$ and the modulus $m(\phi)$ is defined as

$$m(\phi) \equiv \frac{x_2(\phi) - x_3(\phi)}{x_1(\phi) - x_3(\phi)} = \frac{\sin(\phi/3)}{\sin[(\pi + \phi)/3]}. \quad (45)$$

Here, for $-1/2 < E < 0$ (region II), we have $0 < \phi < \pi/2$ and $0 < m < 1/2$, while for $0 < E < 1/2$ (region III), we have $\pi/2 < \phi < \pi$ and $1/2 < m < 1$. For $|E| > 1/2$ (regions I and IV), m is a complex-valued number:

$$m(\psi) = \begin{cases} 1 - \exp[i\chi(\psi)] & (E < -1/2) \\ \exp[i\chi(\psi)] & (E > 1/2) \end{cases} \quad (46)$$

where the phase $\chi(\psi) = 2 \arctan[3^{-1/2} \tanh(\psi/3)]$ vanishes at $\psi = 0$ and reaches $\chi(\infty) = 2 \arctan(3^{-1/2}) = \pi/3$ at $\psi = \infty$. Hence, the relation between m_I (for $E < -1/2$) and m_{IV} (for $E > 1/2$) is $m_I' \equiv 1 - m_I = m_{IV}$, where

$$m'(\phi) \equiv \frac{x_1(\phi) - x_2(\phi)}{x_1(\phi) - x_3(\phi)} = \frac{\sin[(\pi - \phi)/3]}{\sin[(\pi + \phi)/3]}. \quad (47)$$

For energy levels $|E| > 1/2$, we easily verify that $m_{IV}'(\psi) \equiv m_I'(\psi)$.

A. Jacobi elliptic functions

The Jacobi elliptic functions $\text{cn}(z|m)$, $\text{sn}(z|m)$, and $\text{dn}(z|m)$ have real and imaginary periods determined by the complete elliptic integrals of the first kind $K(m)$ and $K'(m) \equiv K(m') = K(1 - m)$, respectively:

$$\left. \begin{aligned} \text{cn}(z + 4nK + 2n'(K + iK')|m) &= \text{cn}(z|m) \\ \text{sn}(z + 4nK + 2n'iK'|m) &= \text{sn}(z|m) \\ \text{dn}(z + 2nK + 4n'iK'|m) &= \text{dn}(z|m) \end{aligned} \right\}, \quad (48)$$

for all integers n and n' . In addition, these functions have zeroes at $\text{cn}(K|m) = 0$, $\text{sn}(0|m) = 0$, and $\text{dn}(K +$

$iK'|m) = 0$, as well as singularities (poles) at $z = iK'$. Lastly, they satisfy the following identities $\text{cn}^2(z|m) + \text{sn}^2(z|m) = 1$, $\text{dn}^2(z|m) + m \text{sn}^2(z|m) = 1$, and have the following limits: $\text{sn}(z|0) = \sin z$, $\text{cn}(z|0) = \cos z$, $\text{dn}(z|0) = 1$, and $\text{sn}(z|1) = \tanh z$, $\text{cn}(z|1) = \text{sech } z = \text{dn}(z|1)$.

The function $y = \text{sn}(z|m)$ satisfies the differential equation

$$(y')^2 = (1 - y^2) (1 - m y^2), \quad (49)$$

the function $y = \text{cn}(z|m)$ satisfies the differential equation

$$(y')^2 = (1 - y^2) (m' + m y^2), \quad (50)$$

and the function $y = \text{dn}(z|m)$ satisfies the differential equation

$$(y')^2 = (1 - y^2) (y^2 - m'). \quad (51)$$

Other Jacobi elliptic functions that will be useful below are $y = \text{sc}(z|m) \equiv \text{sn}(z|m)/\text{cn}(z|m)$, which satisfies the differential equation

$$(y')^2 = (1 + y^2) (1 + m' y^2), \quad (52)$$

and $y = \text{cs}(z|m) \equiv \text{cn}(z|m)/\text{sn}(z|m)$, which satisfies the differential equation

$$(y')^2 = (1 + y^2) (m' + y^2). \quad (53)$$

By comparing Eqs. (49) and (52), for example, we obtain the following identity

$$\text{sn}(z|m') = -i \text{sc}(iz|m), \quad (54)$$

while Eq. (50) yields the identity $\text{cn}(z|m') = 1/\text{cn}(iz|m) \equiv \text{nc}(iz|m)$.

B. Bounded orbit solutions

We begin with bounded orbit solutions in region (II) and (III), where $0 \leq m(\phi) \leq 1$. First, we substitute

$$x^b(t) = x_3 + \alpha y^2(\kappa t) \quad (55)$$

into Eq. (5) to obtain

$$\alpha \kappa^2 (y')^2 = [(x_1 - x_3) - \alpha y^2] [(x_2 - x_3) - \alpha y^2].$$

Next, using the definition (45), we define $\kappa^2 = x_1 - x_3$ and $\alpha = x_2 - x_3 \equiv m \kappa^2$, so that we obtain the differential equation (49), whose solution is $y(\kappa t) = \text{sn}(\kappa t | m)$. Hence, in regions (II) and (III), the bounded orbit solution is

$$x^b(t) = x_3 + (x_2 - x_3) \text{sn}^2\left(\sqrt{x_1 - x_3} t \mid m\right). \quad (56)$$

The bounded separatrix solution is obtained from Eq. (56) in the limit $m \rightarrow 1$:

$$x^{bs}(t) = -1 + \frac{3}{2} \tanh^2\left(\sqrt{\frac{3}{2}} t\right), \quad (57)$$

which is identical to Eq. (38).

Since the Jacobi elliptic function $\text{sn}(z|m)$ has a period $4K(m)$, where $K(m)$ is the complete elliptic integral of the first kind, the period of the orbit solution (56) is

$$\frac{2K(m)}{\sqrt{x_1 - x_3}} = \begin{cases} 2\omega & (0 \leq m \leq 1/2) \\ 2|\omega'| & (1/2 \leq m < 1) \end{cases} \quad (58)$$

For $E = -1/2$, we find $m = 0$, with $x_1 - x_3 = 3/2$ and $x_2 - x_3 = 0$, so that the period (58) is $2K(0)/\sqrt{3/2} = 2\pi/\sqrt{6} = 2\Omega_0$, where we used $K(0) = \pi/2$. In the limit $m \rightarrow 1$ ($E \rightarrow 1/2$), $|\omega'| \rightarrow \infty$ since $K(m) \rightarrow K(1) = K'(0) = \infty$. When $E = 0$ ($m = 1/2$), we find $x_1 - x_3 = \sqrt{3}$ and the period (58) is $2K(1/2)/3^{1/4} = 2\omega_0$.

C. Unbounded orbit solutions

1. Regions (I)-(III)

We now consider the unbounded orbit solutions in regions (I)-(III), where $x^u(0) = x_1$. First, we substitute

$$x^u(t) = x_1 + \alpha/y^2(\kappa t) \quad (59)$$

into Eq. (5) to obtain

$$\alpha \kappa^2 (y')^2 = [y^2(x_1 - x_2) + \alpha] [y^2(x_1 - x_3) + \alpha],$$

where the solution $y(\kappa t)$ must satisfy the initial condition $y(0) = \infty$. Next, using the definition (47), we define $\kappa^2 = x_1 - x_3$ and $\alpha = x_1 - x_2 = m' \kappa^2$, so that we obtain the differential equation (53), whose solution is $y(\kappa t) = \text{cn}(\kappa t|m)/\text{sn}(\kappa t|m)$. Hence, in regions (I)-(III), the unbounded orbit solution is

$$x^u(t) = x_1 + (x_1 - x_2) \frac{\text{sn}^2(\sqrt{x_1 - x_3} t \mid m)}{\text{cn}^2(\sqrt{x_1 - x_3} t \mid m)}. \quad (60)$$

In regions (II) and (III), all roots $x_3 < x_2 < x_1$ are real and $0 < m < 1$. The unbounded orbit solution (60) reaches infinity after a time $K(m)/\sqrt{x_1 - x_3}$ when $\text{cn}(K(m)|m) = 0$. In region (I), where x_1 is real and $x_2 = x_3^*$ are complex-conjugate roots, and the definition (46) for m implies that it is complex-valued.

We note that the unbounded separatrix solution cannot be obtained from Eq. (60) since $x_1 = x_2$ when $E = 1/2$ (or $m = 1$). If we use the initial condition $x^{bu}(0) = \infty$, i.e., $y(0) = 0$, and the definitions $\alpha = x_1 - x_3 = \kappa^2$, we obtain the differential equation (52), whose solution is $y(\kappa t) = \text{sn}(\kappa t|m)/\text{cn}(\kappa t|m)$. Hence, the

unbounded orbit solution in region (III) can also be expressed as

$$x^u(t) = x_1 + (x_1 - x_3) \frac{\text{cn}^2(\sqrt{x_1 - x_3} t | m)}{\text{sn}^2(\sqrt{x_1 - x_3} t | m)}, \quad (61)$$

so that the unbounded separatrix solution becomes

$$\begin{aligned} x^{us}(t) &= \frac{1}{2} + \frac{3}{2} \frac{\text{sech}^2(\sqrt{3/2} t)}{\tanh^2(\sqrt{3/2} t)} \\ &= -1 + \frac{3}{2} \coth^2\left(\sqrt{\frac{3}{2}} t\right), \end{aligned} \quad (62)$$

which is identical to Eq. (41).

2. Region (IV)

In region (IV), where $E > 1/2$, $x_3 < 0$, and $x_1 = x_2^*$, the parameter m is a complex-valued number (46) with unit magnitude $|m| = 1$. The unbounded orbit solution

$$x_{IV}^u(t) = x_3 + (x_2 - x_3) \text{sn}^2\left(\sqrt{x_1 - x_3} t \mid m\right) \quad (63)$$

given by Eq. (56) is still applicable in this region. Using the fact that $\text{sn}(z|m)$ is infinite at $z = iK'(m)$ for $m \neq 0$. Hence, at a finite (complex) time $iK'(m)/\sqrt{x_1 - x_3}$, the particle reaches infinity.

D. Relations between bounded and unbounded orbit solutions

We now wish to verify that the Jacobi orbit solutions derived in this Section satisfy the relations (44) between the bounded and unbounded solutions.

If we use the relation (54), Eq. (63) becomes

$$\begin{aligned} x_{IV}^u(t) &= x_3^{IV} + \alpha_{IV} \text{sn}^2(\kappa_{IV} t | m_{IV}) \\ &= x_3^{IV} - \alpha_{IV} \frac{\text{sn}^2(i\kappa_{IV} t | m_I)}{\text{cn}^2(i\kappa_{IV} t | m_I)} \\ st &= -x_1^I - \alpha_I \frac{\text{sn}^2(i\kappa_I t | m_I)}{\text{cn}^2(i\kappa_I t | m_I)} \equiv -x_I^u(it), \end{aligned} \quad (64)$$

where we used the fact that $m_{IV} = m_I' = 1 - m_I$ and we recover the relation (44). Next, we look at the bounded solution in region (III)

$$\begin{aligned} x_{III}^b(t) &= x_3^{III} + \alpha_{III} \text{sn}^2(\kappa_{III} t | m_{III}) \\ &= -x_1^{II} - \alpha_{II} \frac{\text{sn}^2(i\kappa_{II} t | m_{II})}{\text{cn}^2(i\kappa_{II} t | m_{II})} = -x_{II}^u(it), \end{aligned} \quad (65)$$

and the bounded solution in region (II)

$$\begin{aligned} x_{II}^b(t) &= x_3^{II} + \alpha_{II} \text{sn}^2(\kappa_{II} t | m_{II}) \\ &= -x_1^{III} - \alpha_{III} \frac{\text{sn}^2(i\kappa_{III} t | m_{III})}{\text{cn}^2(i\kappa_{III} t | m_{III})} \\ &= -x_{III}^u(it). \end{aligned} \quad (66)$$

Hence, the relations (44), which were originally obtained through the g_3 -inversion relation (15), are also obtained through the transformation $m \rightarrow m' = 1 - m$, even when m is complex-valued.

VI. SUMMARY

A consistent notation for the half-periods ($\omega_1, \omega_3, \omega_2 \equiv \omega_1 + \omega_3$) of the Weierstrass elliptic function $\wp(z; g_2, g_3)$ was constructed from the analysis of the motion of a particle in a cubic potential. A guide to the accurate interpretation of the Mathematica output for the function $\text{WeierstrassHalfPeriods}(g_2, g_3) = \{\omega_a, \omega_b\}$ was also provided.

-
- [1] W. P. Reinhardt and P. L. Walker, *Weierstrass Elliptic and Modular Functions*, in NIST Handbook of Mathematical Functions (Cambridge University Press, Cambridge, 2010), Chap. 23.
- [2] D. F. Lawden, *Elliptic Functions and Applications*, (Springer-Verlag, New York, 1989).
- [3] A. J. Brizard, *A primer on elliptic functions with applications in classical mechanics*, arXiv:0711.4064v1 (2007).

- [4] A. J. Brizard, *Eur. J. Phys.* **30**, 729 (2009).
- [5] A. J. Brizard, *An Introduction to Lagrangian Mechanics*, 2nd ed. (World Scientific, 2015), App. B.
- [6] W. P. Reinhardt and P. L. Walker, *Jacobian Elliptic Functions*, in NIST Handbook of Mathematical Functions (Cambridge University Press, Cambridge, 2010), Chap. 22.